SIZE EFFECT TESTS AND FRACTURE CHARACTERISTICS OF ALUMINUM

ZDENĚK P. BAŽANT,† SOO-GON LEE‡ and PHILLIP A. PFEIFFER§

Center for Concrete and Geomaterials, Northwestern University, Evanston, IL 60201, U.S.A.

Abstract— The recently established approximate size effect law for blunt fracture is shown to agree with test data for aluminum. The data are obtained with three-point bent fracture specimens of depths ranging from 0.25 to 4 in. Non-linear fracture parameters can be obtained by a linear regression based on the size effect law. Thus, the fracture energy can be determined using only the maximum load values from fracture tests, and the R-curve can be obtained as an envelope of fracture equilibrium curves. No measurements of crack length or specimen compliance are needed.

INTRODUCTION

FRACTURE of aluminum generally does not follow linear elastic fracture mechanics. This means that a non-linear fracture model must be used. One conspicuous consequence of the non-linearity of fracture properties is the apparent variation of the energy required for crack growth, R, with the length of the crack. Irwin[1] and Krafft *et al.*[2] proposed that the dependence of R on the crack length, c, may be considered to be approximately the same for various fracture geometries. This means that one can use for fracture calculations a unique curve, $R(c)$, called the R-curve (resistance curve), which is considered to be a material property.

The existing methods for determining the R-curve, specified by an ASTM standard [3–6], rely on the relation $R = k_1 P^2 a/(E_c b^2 d^2)$ in which e_c = Young's elastic modulus, b = specimen thickness, d = characteristic dimension of the specimen, a = length of the crack plus notch, P = load at which the crack extends and k_1 = a coefficient determined for the given specimen geometry according to linear elastic fracture mechanics. A series of R-values is measured, either on a single specimen for various crack lengths corresponding to various loads, P, or on a series of specimens from the critical values of P and the corresponding crack lengths. In each case, the crack lengths must be determined, either by direct measurements or indirectly by measurements of the specimen's compliance at unloading or reloading. The need to measure the crack length is a considerable obstacle, first because the location of the crack tip is not easy to define, and second because the visible crack length is not the most relevant information for the use of the R-curve in structural analysis. For that purpose, the crack length should ideally represent the length of a certain equivalent crack that yields the correct remote elastic stress field, rather than the actual crack length in the non-linear material. Another drawback of determining the R-curve on a single specimen (or specimens of the same kind) is the fact that only one point on the R-curve actually corresponds to a critical state of the specimen (i.e. to failure under load control).

If the R-curve should be used for predicting failure loads (maximum loads) of structures, it is certainly more desirable, as well as simpler, to use data on the failure loads alone. This is made possible by using specimens of different sizes for which the failure occurs at different crack lengths. A method of this type, similar to a method previously developed for concrete[7], will be proposed in this paper. It will make use of the size effect and the salient characteristics of fracture mechanics. The effect of specimen size on the apparent fracture toughness values has been investigated before [8, 9]; however, it has not been exploited for determining the non-linear fracture properties.

SIZE EFFECT LAW

The size effect can be exploited because an approximate but quite general size effect law, which can be used for smoothing and extrapolating the data from specimens of various sizes, has

been recently established[10]. It has already been applied with success for concrete and reinforced concrete[7, 11]. However, this law is not restricted to concrete alone and should hold as an approximation for non-linear fracture with crack blunting in general[10].

Consider geometrically similar specimens or structures with geometrically similar notches, having the same thickness, b, and made of the same material. For the purpose of determining the size effect, one may introduce the following approximate hypothesis. The total energy, W, dissipated due to fracture depends on: (1) the length a of the crack and (2) the size of the fracture process zone, d_f, which is assumed to be constant at failure state.

Consequently, W must be a function of two non-dimensional parameters a/d and d_f/d, and dimensional analysis with similitude arguments then leads[12] to the following size effect law[10]:

$$\sigma_N = Bf_y \left(1 + \frac{\lambda}{\lambda_0}\right)^{-1/2}, \qquad \lambda = \frac{d}{d_f}, \tag{1}$$

in which $\sigma_N = P/bd$ = nominal stress at failure, P = maximum load (i.e. failure load), d = characteristic dimension of the specimen or structure (e.g. the beam's depth), f_y = uniaxial yield stress, λ = relative structure size and B, λ_0 = two empirical constants which depend on the geometrical shape of the specimen or structure but not on its size. In the graph of log σ_N vs log d, eqn (1) is plotted in Fig. 1.

If the structure is very small ($\lambda \to 0$), then the second term in the parentheses in eqn (1) is negligible compared to 1, therefore $\sigma_N = Bf_y$ = const. This limit case, in which there is no size effect, represents the yield criterion of failure and corresponds to a horizontal line in Fig. 1. If the structure is very large ($\lambda \to \infty$), then 1 is negligible compared to the second term in the parentheses of eqn (1), and then $\sigma_N \simeq \text{const}/\sqrt{d}$. This is the size effect typical of linear elastic fracture mechanics; it corresponds to the inclined straight line in Fig. 1, having the slope $-1/2$. In general, the size effect law according to eqn (1) represents a gradual transition from the yield criterion for very small structures to the energy criterion of linear elastic fracture mechanics for very large structures.

For smoothing and extrapolation of the measured raw data as well as their statistical analysis, it is important that the size effect law from eqn (1) can be transformed to a linear regression plot
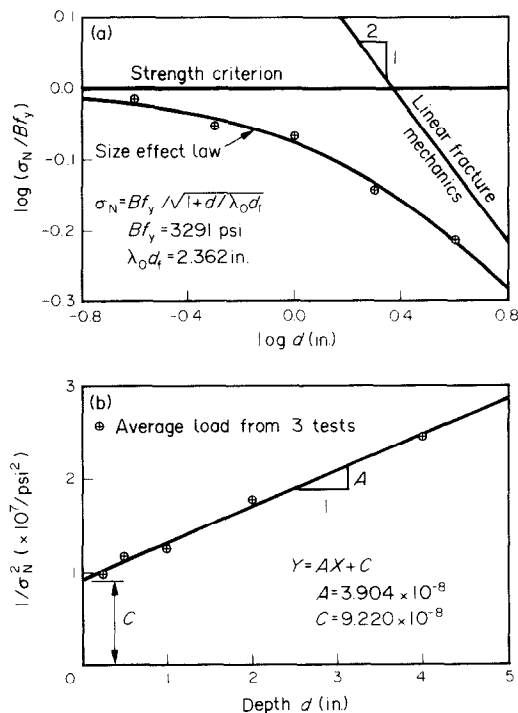

Fig. 1. The size effect law, its linear regression and comparison with test data for aluminum.

of the form:

$$Y = AX + C \tag{2}$$

in which

$$X = d, \qquad Y = \frac{1}{\sigma_N^2} = \left(\frac{bd}{P}\right)^2, \qquad A = \frac{C}{\lambda_0 d_f}, \qquad C = \frac{1}{B^2 f_y^2}, \tag{3}$$

A is the slope of the regression line [Fig. 1(b)] and C is the Y-intercept. Plotting the measured failure data for geometrically similar specimens of different sizes in this regression plot, one can obtain easily A and C by least-square regression. After determining A and C by linear regression, we have $B = \sqrt{C/f_y}$, $\lambda_0 = C/(Ad_f)$.

DETERMINATION OF FRACTURE ENERGY FROM SIZE EFFECT MEASUREMENTS

Let c represent the length of the crack from the tip of the notch and a_0 represent the length of the notch; let $a = a_0 + c$. For a larger specimen, the crack length c at failure is normally longer. However, the crack length at failure is bounded by a certain ratio to the size of the fracture process zone, and therefore, for very large specimens, the relative crack length at failure, $\alpha = c/a_0$, is essentially constant. Thus, in the limit $d \to \infty$, for which $a_0 \to \infty$, the value of the relative crack length α approaches $\alpha_0 = a_0 d$. At the same time, for very large specimens, the size of the fracture process zone becomes negligible compared to the size of the specimen, and so linear elastic fracture mechanics must apply in the limit. Thus, for very large specimens:

$$\sigma_N = \sqrt{\frac{G_f E}{g(\alpha_0)d}} \tag{4}$$

in which $g(\alpha_0)$ is the non-dimensional energy release rate according to linear elastic fracture mechanics for a crack of length a_0. The value of $g(\alpha_0)$ is known for many typical specimen geometries and is found in textbooks and handbooks[13]. The value of $g(\alpha_0)$ can always be determined by linear finite element analysis.

According to the size effect law [eqn (1)], for very large d we have

$$\sigma_N = Bf_y \sqrt{\frac{\lambda_0 d_f}{d}}. \tag{5}$$

Now, equating expressions for σ_N [eqns (4) and (5)] and solving for fracture energy G_f, we obtain the basic result[7]:

$$G_f = \frac{g(\alpha_0)}{AE}. \tag{6}$$

Thus we see that the fracture energy is inversely proportional to the slope of the size effect regression line [Fig. 1(b)]. This provides a convenient method of determination of fracture energy.

DETERMINATION OF R-CURVE FROM SIZE EFFECT MEASUREMENTS

The size effect law is also helpful for determining the R-curve[7]. In terms of the R-curve $R(c)$, which describes the dependence of the energy required for crack growth on the crack length measured from the notch tip, the energy balance condition requires that

$$G(a) = R(c) \qquad (a = a_0 + c), \tag{7}$$

in which $G(a)$ is the energy release rate according to an equivalent linear elastic analysis. The foregoing relation may be regarded as an equilibrium relation for fracture. The equilibrium may be stable, critical or unstable. The critical state is the state at maximum load P_{max}. The condition of stability of fracture is known to have the form:

$$\frac{dR(c)}{dc} - \frac{dG(a)}{da} \geq 0 \text{ (stable)} \tag{8}$$

$$= 0 \text{ (critical)}.$$

The energy release rate according to linear elastic fracture mechanics has always the form $G(a) = P^2 g(\alpha)/(Eb^2 d)$, and so for the maximum measured loads we have

$$G(a) = \frac{P_{max}^2 g(\alpha)}{Eb^2 d} \quad \left(\alpha = \frac{a}{d}\right), \tag{9}$$

in which $g(\alpha)$ is a function available in handbooks for typical specimen geometries[13] and obtainable in general by linear finite element analysis.

According to eqns (7)–(8), failure occurs when the curve $G(a)$ has the same value and the same slope as the curve $R(c)$. Consequently, the R-curve represents the envelope of all curves $G(a)$, plotted according to eqn (9) for various measured values of maximum load, P_{max}.

Thus, the R-curve may be obtained from size effect tests if the curve $G(a)$ is plotted for each specimen size and the corresponding maximum load, using the known function $g(\alpha)$. In practice, a problem arises however for two reasons: (1) the test data exhibit statistical scatter and (2) the range of measured data is usually insufficient for determining the complete envelope.

To avoid these difficulties, we must take recourse to the size effect law [eqn (1)].If the raw, scattered values of P_{max} are used to plot the curves $G(a)$ for various specimen sizes, no common envelope can be obtained [Fig. 2(b)]. Thus, smoothing of the measured data according to the size effect law is required before the R-curve can be determined. Furthermore, if the curves $G(a)$ are plotted only for a limited range of measured P_{max}-values, determination of the R-curve is ambiguous, as illustrated in Fig. 2(c). It is necessary to plot the curves $G(a)$ for P_{max}-values within a range of $1:100$ or more, and such a range can hardly be obtained except by generating the P_{max}-values from the size effect law [eqn (1)] after parameters B and λ_0 have been determined by regression of the test data.

The R-curve can be also constructed, in principle, according to the failure load for different notch lengths on specimens of the same size. However, this method fails for the same reason as mentioned; the range of the curve $G(a)$ is insufficient, like in Fig. 2(c). The R-curve can be obtained from such data only if additional properties, such as the crack length or the specimen compliance, are measured. However, this has the drawback already stated, in particular the fact that load values which do not correspond to failure states must be also included in the evaluation.

It has been shown[7] that the R-curve obtained from test data smoothed by the size effect law in eqn (1) is very closely approximated by the formula

$$R(c) = G_f\left[1 - \left(1 - \frac{c}{c_m}\right)^n\right] \quad \text{for} \quad c \leq c_m, \qquad R(c) = g_f \quad \text{for} \quad c > c_m, \tag{10}$$

in which G_f is already known in advance from eqn (6) and parameters c_m and n are to be identified by fitting of the envelope. Usually, as a good approximation, $n = 3.6$.

It must be kept in mind that the R-curve is an approximate concept. In theory, the R-curves for different specimen geometries should not be the same; however, experience has shown that in many situations the R-curves are nearly the same, while in others they are not[7].

FRACTURE TESTS OF ALUMINUM

After initial success with concrete[7], the new test procedure outlined here has been applied to aluminum Al 6061-T651 (a product of Alcoa Co.). Three-point bent fracture specimens have been
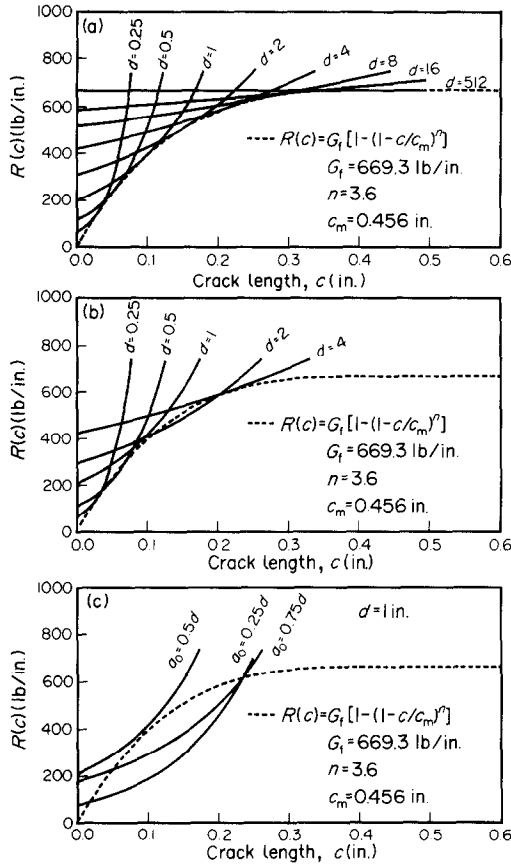
Fig. 2. (a) R-curve obtained as an envelope of fracture equilibrium curves for smoothed maximum loads. (b) Fracture equilibrium curves plotted for unsmoothed maximum load data. (c) Fracture equilibrium curves for specimens with different notch lengths but same size, and ambiguity of the R-curve.

used; their geometry and the detail of the notch are given in Fig. 3. The notch, which has one of the ASTM standard shapes, has been machined very carefully, especially its sharp tip formed by plane surfaces of 30° inclination. The specimens were tested at a temperature of 75°F in an MTS closed-loop testing machine. Three tests have been made for each specimen size and shape, and their reproducibility was excellent (Table 1). The typical load deflection diagram recorded in the MTS machine is shown in Fig. 4, and as mentioned only the peak value has been used for further analysis. The values of the maximum loads obtained for geometrically similar specimens of various sizes appear in rows A–E of Table 1. The table also lists the averages for each group of three specimens and the smoothed values from the size effect law [eqn (1)]. The average $\bar{P}_{\max}$-values are used to plot the data points in the size effect plot in Fig. 1(a), as well as the regression plot in Fig. 1(b). The slope and the intercept of the regression line are $A = 3.904 \times 10^{-8}$ in.^{2}/lb. and $C = 9.220 \times 10^{-8}$ in. lb.
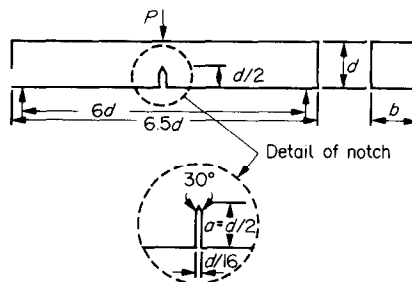

Fig. 3. Geometry of the test specimen and detail of the notch.

Table 1. Parameters of fracture tests and test results

Type	b (in.)	a/d	d (in.)	P_{max} (lb)			Average $\bar{P}_{max}$	Smoothed P_{max}	Displacement rate $10^{-7}\delta$	Time to failure (s)
A	1	0.5	0.25	792	800	802	798	783	595	392
B	1	0.5	0.5	1450	1458	1476	1461	1496	945	511
C	1	0.5	1	2848	2768	2872	2829	2760	1500	500
D	1	0.5	2	4731	4751	4761	4748	4948	2300	536
E	1	0.5	4	7936	8061	8200	8066	8026	3800	649
F	1	0.75	1	660	664	670	665	—	1500	667
G	1	0.25	1	5110	5130	5140	5127	—	1500	578
H	0.75	0.5	1.5	2850	2866	—	—	2897	—	—

Tada *et al.*'s handbook[13] gives the values of $g(\alpha)$ only for specimen length–depth ratios 8 and 4, while 6 was used in the present tests. Therefore, linear interpolation has been used between the values for $L/d = 8$ and 4, which has led to the value $g(\alpha_0) = 261.3$. With Young's modulus $E = 1.0 \times 10^7$ lb/in.^{2} and $A = 3.904 \times 10^{-8}$, eqn (6) yields the fracture energy

$$G_f = 669 \text{ lb/in.} = 117 \text{ kN/m.} \tag{11}$$

The smoothed values of the maximum loads of specimens of various sizes are listed also in Table 1 in rows A–E. From these values, the R-curve is constructed as an envelope, as shown in Fig. 2. If the raw, unsmoothed average measured values of the maximum loads were used, the fracture equilibrium curves for the measured data would be as shown in Fig. 2(b), from which determination of the R-curve as an envelope is ambiguous.

The machine's displacement rate in these tests was varied as indicated in Table 1, so as to ensure that the times to reach the maximum load (also given in Table 1) were roughly the same for all the specimen sizes.

The thickness of the specimens of all sizes in the foregoing tests has been the same, $b = 1$ in. (Table 1). The thickness of the specimen could be important because of the differences between the plane states of stress and of strain, and because of differences in plastic yielding around the fracture front. The elastic Poisson effect, and even more plastic yielding in transversely inclined planes, causes lateral deformations around the crack tip, which are clearly visible as deformations of the surface (see Fig. 5). This phenomenon, called the shear lip[6], means that the front edge of the crack across the thickness of the plate is not straight but has a V-shape, as has been confirmed by observing the fracture surfaces on fully broken specimens. These phenomena are part of the fracture blunting process which render linear elastic fracture mechanics inapplicable, so that non-linear fracture mechanics, such as the present analysis, must be used.

It seems that the comparability of specimens of different sizes is best when the thicknesses of all the specimens are the same. This is true, however, only with regard to the plastic yielding phenomenon. With regard to the effect of the Poisson ratio, the consequence of which is an additional surface singularity[14] caused by the fact that the plane strain state prevailing at mid-thickness of
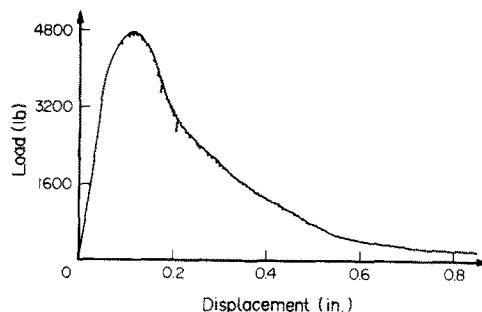

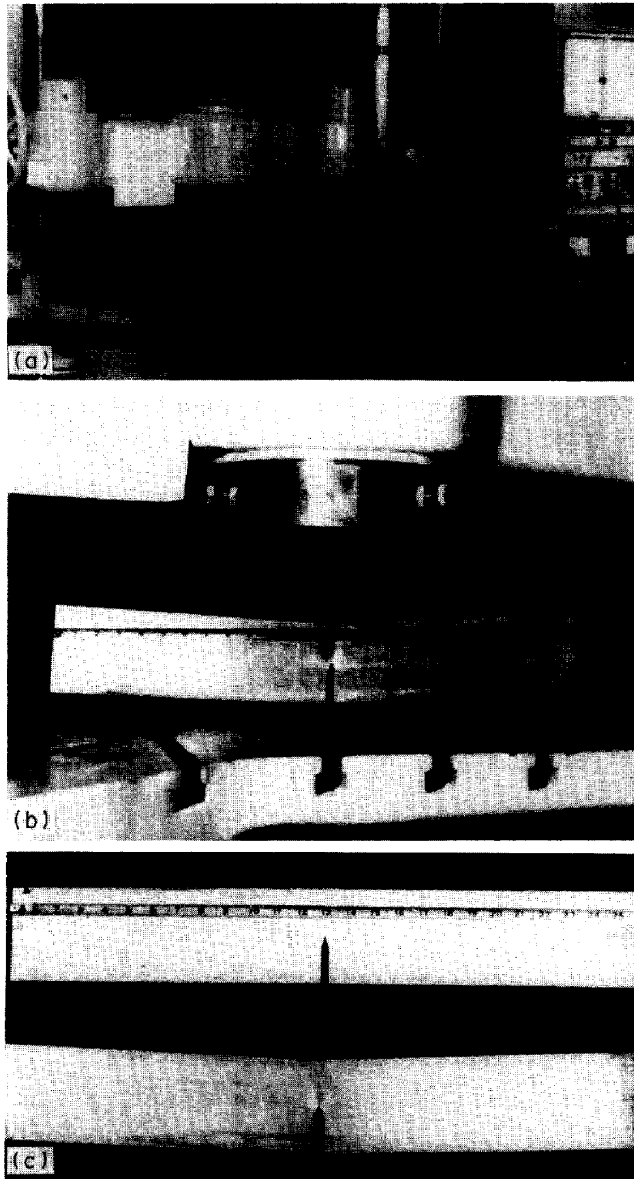Fig. 4. Typical load–deflection diagram recorded in the MTS machine.

Fig. 5. (a) Photo of the testing machine with the test specimen. (b) Test specimen during loading. (c) Fracture specimen before testing and after testing to maximum load.
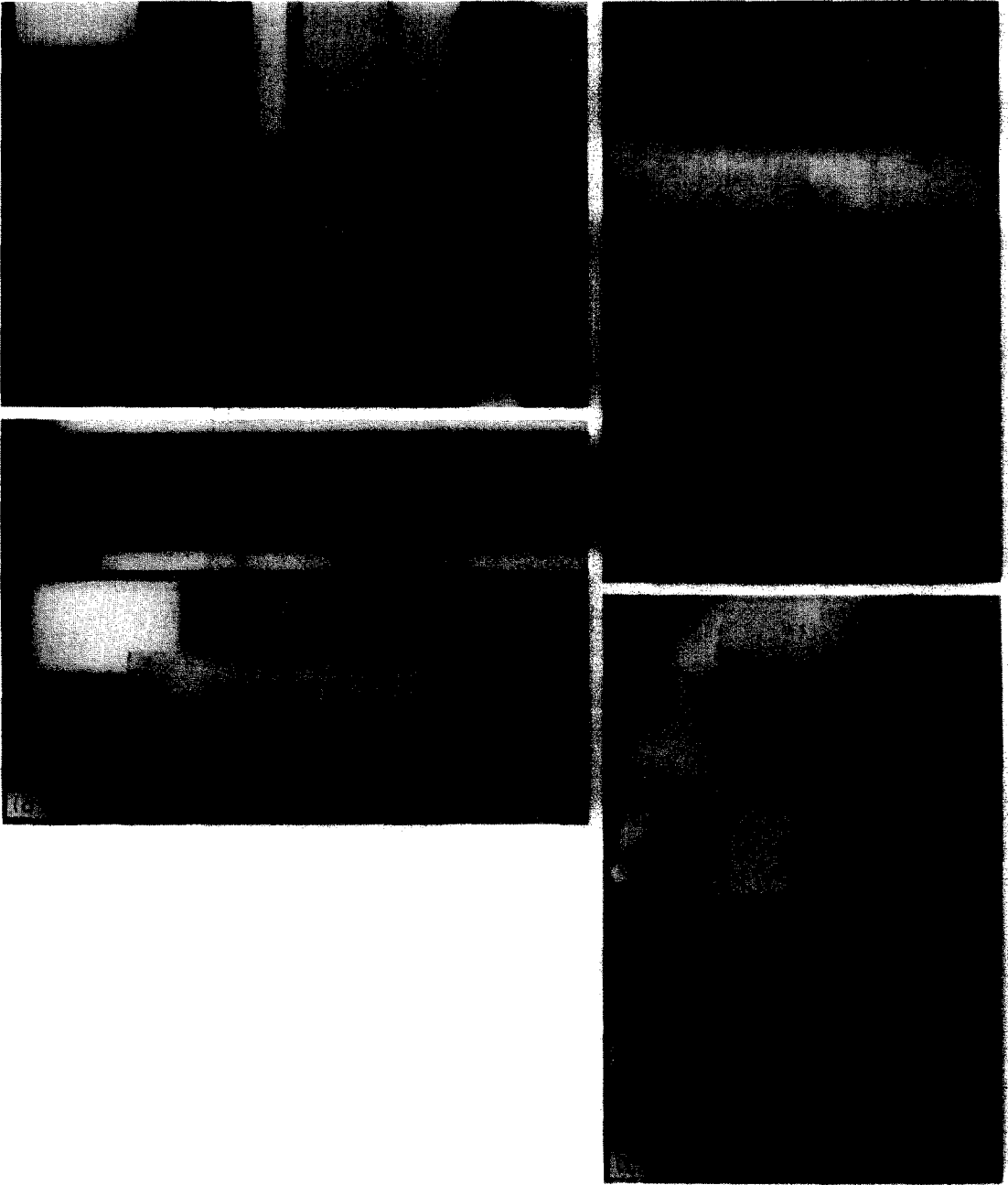
Fig. 7. (a) Test set-up in Instron Machine. (b) test specimens of different sizes. (c) Close-ups of notch (bottom) and of fracture zone (top).
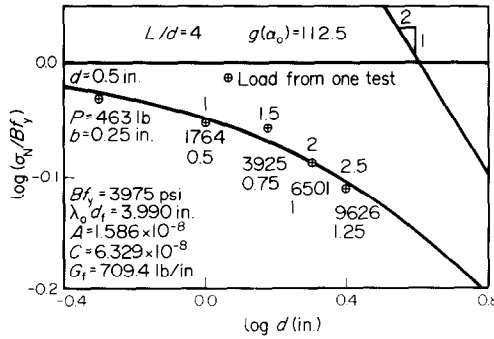
Fig. 6. Size effect plot of test results of specimens with proportional thicknesses.

the specimen does not match the surface boundary conditions, it might possibly have been better for comparability of specimens of different sizes to use thicknesses proportional to beam depth. However, this was not done because the elastic effects seem less important. Nevertheless, in a preliminary test one beam of different thickness, $b = 0.75$ in., has been tested, and the results (row H in Table 1) are still essentially in agreement with the values of σ_N for the size effect law, based on rows A–E.

A few tests have been also carried out for a fixed specimen size ($d = 1$ in.) and different notch lengths, $a/d = 0.25, 0.5$ and 0.75 (rows G, A and F in Table 1). The fracture equilibrium curves for the measured maximum loads (Table 1) are plotted in Fig. 2(c), and it is clear that determination of the R-curve as an envelope is totally ambiguous for such a set of measurements, as already emphasized. So a single specimen size cannot be used unless more than just the maximum load is measured, as is well known.

The foregoing tests have been carried out at Northwestern University. A further test series has been carried out at Chonnam National University, to check the effect of scaling in which the thickness is varied in proportion to the beam depth and length. The results of these tests, carried out with an Instron machine, are given in Figs 6 and 7 where the maximum loads are indicated next to the points of σ_N. The fracture energy value obtained by smoothing with the size effect law is for these tests $G_f = 709$ lb/in., which is only 6.0% larger than in the previous tests with constant specimen thickness. From this it seems that the question of how the thickness should be scaled is not very important.

CRACK BAND FINITE ELEMENT MODEL

Fracture behavior which follows the size effect according to eqn (1) can be closely modeled in finite element analysis using the crack band theory[15, 16]. The fact that this size effect law is obtained from the hypothesis that the fracture process zone has a certain fixed effective width[10] means that the fracture can be modeled as a band of progressively cracking elements of the same width, h. The material in the finite elements is assumed to exhibit a stress–strain relationship with gradual strain softening, for example as shown in Fig. 8. A simple triaxial constitutive relation which yields the stress–strain diagram with strain softening shown in Fig. 8 has been formulated[16]. The size of the finite element, which represents the effective width of the fracture process zone at the fracture front, may be expressed as
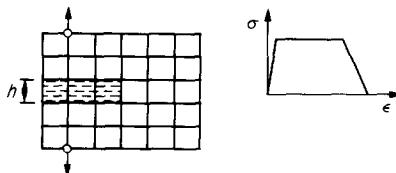
$$h = G_f/W_0, \tag{12}$$

Fig. 8. Finite element crack band model and tensile stress–strain diagram with yield and strain softening.

in which W_0 represents the area under the complete tensile stress–strain diagram with strain softening (Fig. 8). The length of the yield plateau and the strain-softening slope E_t in Fig. 8 govern chiefly the length of the fracture process zone ahead of the crack tip, and E_t can be determined if this length is known.

It is important to realize that a certain precise element size, as given by eqn (12), is required. However, in situations where this would lead to an excessively large number of elements, larger finite elements may be used, but then the slope of the declining segment of the stress–strain curve, and possibly also the peak stress value, must be adjusted so that the product of the area under the complete tensile stress–strain curve with the element width used would give the correct value of fracture energy G_f. Then the results are approximately the same as those for the correct finite element size given by eqn (12).

It has been demonstrated[16] that a finite element model of this type gives the correct size effect curve as shown in Fig. 1 and described by eqn (1), and generally agrees with a wide range of data on non-linear fracture of various materials, including the effect of the notch length on the maximum load and on the variation of energy required for crack growth as a function of the length of the crack from the notch tip, i.e. the R-curve.

Note that the correct R-curve is obtained from the finite element model even though only one constant value of fracture energy, G_f, is used in the model. This value of fracture energy coincides with the energy release rate only in those situations where the ligament cross-section is much larger than the fracture process zone, so that the fracture process zone can fully develop and does not interfere with the boundaries of the structure. If the structure is smaller, then the full size of the fracture process zone cannot develop, and interference with the boundaries occurs, e.g. when finite elements that undergo strain softening are close to the notch tip or to the end of the ligament. This is why the model, with its fixed fracture energy value, is capable of representing the R-curve.

It may be noted that the limiting case in which the tensile stress–strain relation is considered as elastic, followed by a sudden stress drop to zero as the strength limit is reached, yields solutions which are approximately in agreement with linear elastic fracture mechanics provided there are about 15 or more finite elements across the ligament. This is because, for a sudden stress drop, the fracture process zone (elements that undergo cracking) is always limited to a single element width, so that the fracture process zone is localized to the maximum possible within the finite element mesh. This fact also shows that it is not necessary to model fracture in finite element codes as a line interelement crack with a sharp tip. In fact, solutions with a crack band and a sudden stress which drops to zero come as close to the linear elastic fracture mechanics solutions as do the solutions with a sharp interelement crack. The crack band approach to fracture modeling seems to be more flexible, easier to program and also permits modeling fracture in any direction as a zigzag band of crack elements. So far this technique has been used widely only for concrete and geomaterials; however, it may have a potential for non-linear fracture modeling in metals.

GENERALIZED SIZE EFFECT LAW

Equation (1) is the simplest possible approximation to the size effect for non-linear fracture. The most general size effect law may be written in the form of asymptotic expansion[16]:

$$\sigma_N = Bf_y\left[\left(\frac{\lambda_0}{\lambda}\right)^{-r} + 1 + \left(\frac{\lambda_1}{\lambda}\right)^2 + \left(\frac{\lambda_2}{\lambda}\right)^2 + \left(\frac{\lambda_3}{\lambda}\right)^4 + \ldots\right]^{-1/2r}, \tag{13}$$

where f_y, B, r, λ_0, λ_1, λ_2, λ_3, ... are material constants. The first order approximation, obtained by setting $\lambda_1 = \lambda_2 = \lambda_3 = \ldots = 0$, i.e.

$$\sigma_N = Bf_y\left[1 + \left(\frac{\lambda}{\lambda_0}\right)^2\right]^{-1/2r}, \tag{14}$$

is considerably more flexible than eqn (1) for describing various possible shapes of the curve of $\log \sigma_N$ vs $\log \lambda$ which may be obtained by finite element calculations. In fact, finite element experience indicates[17] that more than the first two terms from eqn (13) are never really needed.

In the fitting of available test data, however, coefficient r in eqn (14) cannot be determined unambiguously because of the random scatter of test results and the usual limitations of the size range. Tests over a very broad size range would be required to determine r, in addition to B and λ_0. Nevertheless, if sufficient data are given, then eqn (14) may be also easily used to determine the fracture parameters of the material. Either a non-linear optimization subroutine such as the Marquardt–Levenberg algorithm may be used to determine B, λ_0, and r simultaneously, or eqn (14) may be algebraically rearranged to the linear relation in eqn (2) in which, instead of eqn (3),

$$X = d^r, \qquad Y = \sigma_N^{-2r}, \qquad A = C(\lambda_0 d_f)^{-r}, \qquad C = (BF_y)^{-2r}. \tag{15}$$

A set of r-values, e.g. 1, 0.8, 0.6, 0.4, may be selected and, for each, one finds A and C as well as the sum of squared deviations from the test data by linear regression. Considering the dependence of this sum on r, one may identify the r-value that minimizes this sum. Then $B = C^{-1/2r}/f_y$, $\lambda_0 = (C/A)^{1/r}/d_f$.

For $d/d_f \to \infty$, eqn (14) reduces again to eqn (5). Thus, the fracture energy is again given by eqn (6), although for a different r a different G_f will be obtained.

COMPARISON WITH R-CURVES BASED ON ASTM STANDARD

According to ASTM Standard Recommendation E561-81, the R-curve is determined from compliance measurements on a single compact tension specimen of the type shown in Fig. 9. These tests have been also carried out using three groups of specimens of different sizes (specified in the Table in Fig. 1). The crack opening displacement, COD, was measured by a clip gage with an accuracy of 10^{-6} m and base length under $w/4$, mounted at distance $(0.1576 \pm 0.0006)w$ ahead of
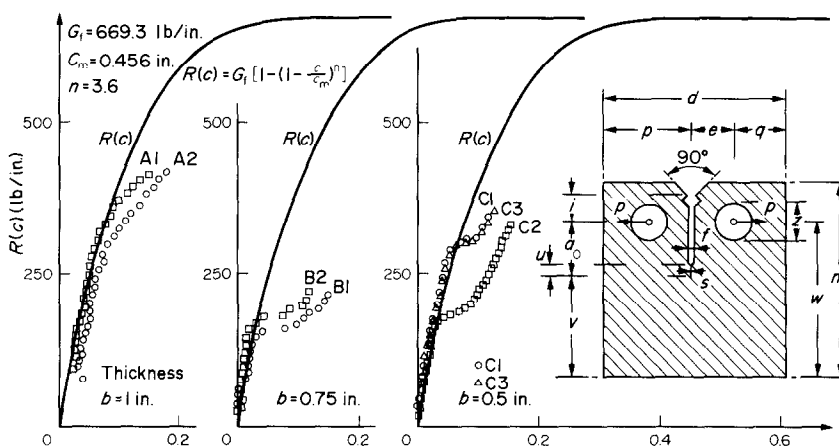

Fig. 9. Comparison with R-curves obtained by ASTM procedure based on compact tension specimens (solid curve = R-curve from present method).

Dimensions (in., except s, mm)

Specimen	b	d	e	f	i	m	p	q	u	v	z
A1, A2	1.00	2.4	0.550	0.18	0.314	2.500	1.2	0.650	0.20	1.2	0.500
B1, B2	0.75	1.8	0.413	0.118	0.236	1.875	0.9	0.488	0.15	0.9	0.375
C1, C2, C3	0.50	1.2	0.275	0.098	0.157	1.250	0.6	0.325	0.10	0.6	0.250

	A1	A2	B1	B2	C1	C2	C3
t	0.998	0.994	0.748	0.744	0.498	0.498	0.498
w	2.004	2.004	1.496	1.496	0.976	0.992	0.996
a_0	0.819	0.803	0.628	0.628	0.386	0.407	0.406
s	0.13	0.13	0.13	0.13	0.30	0.13	0.30 mm

the axis connecting the centers of the loading pins (for w see Fig. 9). The initial notch was cut with a saw and, instead of producing a fatigue crack, a slit crack extending from the notch tip was machined by a diamond disc paper of thickness 0.13 or 0.30 mm (see the table in Fig. 1). The cross-head speed of the machine was 0.2 mm/min.

The R-curve points obtained from these tests are shown in Fig,. 1. They were obtained by the following procedure. Take representative points on the recorded graph of load P vs $2v_1 = $ COD. Calculate the values of $2v_1 Eb/P$ and find the equivalent crack length a_e from the compliance table (ASTM E561-81, Table 2). Then calculate $R(c) = K_{cr}^2/E$ (for plane stress) where $K_{cr} = Pb^{-1}w^{-1/2}f(\xi)$ [13, 18, 19] where $\xi = a_e/w$,

$$f(\xi) = (0.866 + 4.64\xi - 13.32\xi^2 + 14.72\xi^3 - 5.6\xi^4)[(2+\xi)/(1-\xi)^{3/2}]. \tag{16}$$

Then evaluate crack length increments, $c = a_e - a_0$, and finally plot $R(c)$. (The value of K_{cr} for the specimens 1 in., 0.75 in. and 0.5 in. thick were 61,390, 41,940 and 54,040 lb × in.$^{-3/2}$, respectively.)

The curves obtained from the size effect by the present method [eqn (10)] are plotted as the solid curves in Fig. 9. We see that the agreement is initially good, but for longer crack lengths, c, the ASTM method consistently gives significantly lower values of the energy required for crack growth, $R(c)$. These differences, however, are not surprising. In the present method, only maximum load states are used while in the ASTM method only one of the points used is a maximum load state. The fracture process zone size at other than maximum load state may be quite different. Especially, when post-peak load states are considered, the remaining ligament becomes small and the fracture process zone interacts with the specimen boundaries more than it does at maximum load. This might reduce the fracture process zone size and thus cause less energy to be dissipated, which might explain why the values of $R(c)$ at large c are less for the ASTM method.

On the other hand, it should be pointed out that if the generalized size effect law in eqn (14) with $r < 1$ were used, the corresponding R-curve would differ from that plotted in Fig. 9 and would have a lower asymptotic value at large c. The difference from the results of the ASTM method would then be smaller. However, since the ASTM method is based on a specimen of one size, it is unlikely to give adequate information for the full range of the R-curve. This has been demonstrated for concrete in[7].

CONCLUSIONS

(1) The size effect law in eqn (1) or eqn (14) makes it possible to determine fracture energy and other non-linear fracture parameters by measuring only maximum loads of fracture specimens.

(2) The test data from fracture tests of aluminun specimens of different sizes agree with the size effect law.

(3) One advantage of exploiting the size effect law is that statistically scattered measurements are smoothed with a known law permitting linear regression, and that the range of the measured data is thereby extended. The possibility of linear regression is also advantageous for statistical treatment.

(4) Measuring only the maximum loads for specimens with different notch lengths but the same size is insufficient for determining the fracture energy and other non-linear fracture properties.

(5) The initial R-curve for short cracks agrees quite well with the R-curve obtained by the ASTM procedure based on compliance measurements on a single compact tension specimen. For longer cracks, however, the ASTM procedure yields smaller R-curve values, and it provides no information on the final asymptotic value of the R-curve.

In[20] it is experimentally demonstrated that the present method yields approximately the same fracture energy values when specimens of very different geometries are used.

REFERENCES

[1] G. R. Irwin, Report of a Special Committee, Fracture testing of high strength sheet material. *ASTM Bull.*, p. 29, (January 1960) [also G. R. Irwin, Fracture testing of high strength sheet materials under conditions appropriate for stress analysis. Report No. 5486, Naval Research Laboratory July (1960)].

[2] J. M. Krafft, A. M. Sullivan and R. W. Boyle, Effect of dimensions on fast fracture instability of notched sheets. *Cranfield Symp. 1961*, Vol. 1, pp. 8–28.

[3] *1978 Annual Book of Standards*, Part 10, pp. 589–607 (ASTM).

[4] T. T. Shih, An evaluation of the chevron V-notched bend bar fracture toughness specimen. *Engng Fracture Mech.* **14**, 821–832 (1981).

[5] V. Weiss and M. Sengupta, Ductility, fracture resistance, and *R*-curves. *Mechanics of Crack Growth, ASTM STP* **590**, 294–207 (1976).

[6] S. T. Rolfe and J. M. Barsom, *Fracture and Fatigue Control in Structures*, pp. 537–557. Prentice-Hall, Englewood Cliffs, New Jersey (1977).

[7] Z. P. Bažant, J. K. Kim and P. Pfeiffer, Nonlinear fracture properties from size effect tests. *J. struct. Engng ASCE* **112**, 289–307 (1986).

[8] W. Seidel, Specimen size effects on the determination of K_{IC} value in the range of elastic–plastic material behavior. *Engng Fracture Mech.* **12**, 581–597 (1979).

[9] F. G. Nelson, P. E. Schilling and J. G. Kaufman, The effect of specimen size on the results of plane-strain fracture toughness test. *Engng Fracture Mech.* **4**, 33–50 (1972).

[10] Z. P. Bažant, Size effect in blunt fracture: concrete, rock, metal. *J. Engng Mech. ASCE*, **10**, 518–535 (1984).

[11] Z. P. Bažant and J. K. Kim, Size effect in shear failure of longitudinally reinforced beams. *J. Am. Concr. Inst.* **81**, 456–468 (1984).

[12] Z. P. Bažant, Fracture mechanics and strain-softening of concrete. Preprints, *U.S.–Japan Workshop on Finite Element Analysis of Reinforced Concrete*, Tokyo May 1985.

[13] H. Tada, P. C. Paris and G. R. Irwin, *The Stress Analysis of Cracks Handbook*. 2nd ed. Del Research Corp., Hellertown, Pennsylvania (1985).

[14] Z. P. Bažant and L. F. Estenssoro, Surface singularity and crack propagation. *Int. J. Solids Structures* **15**, 405–426 (1979); **16**, 479–481 (1980).

[15] Z. P. Bažant, Fracture mechanics and strain softening of concrete, in *Finite Element Analysis of Reinforced Concrete, Proc. U.S.—Japan Seminar*, Tokyo, May 1985. ASCE, New York (in press).

[16] Z. P. Bažant and B. H. Oh, Crack band theory for fracture of concrete. *Mater. Struct.* **16**, 155–177 (RILEM, Paris, 1983).

[17] Z. P. Bažant, Comment on Hillerborg's comparison of size effect law with fictitious crack model. *Dei Poli Anniversary Volume* (Edited by L. Cedolin). Politecnico di Milano, 335–338 (October 1985).

[18] J. F. Knott, *Fundamentals of Fracture Mechanics*. Butterworth, London (1973).

[19] O. Broek, *Elementary Engineering Fracture Mechanics*. Sijthoff and Noordnoff, Alphen aan den Rijn, The Netherlands (1978).

[20] Z. P. Bažant and P. A. Pfeiffer, *Determination of fracture energy from size effect*. Report No. 86-8/428d, Center for Concrete and Geomaterials, Northwestern University, Evanston, IL, U.S.A. (Sept. 1986).